Chapter

Removal of Methylene Blue Dyes from Aqueous System Using Composite Polymeric-Apatite Resins

Nasser S. Awwad, Adel A. El-Zahhar and Jamila A.M. Alasmary

Abstract

Removal of cationic dyes from industrial effluents is still a big and challenging subject in the field of environmental purification. Millions of tons of cationic dyes are consumed by the textile, rubber, paper, and plastic industries. These dyes have thousands of different chemical structures. Most of them have special properties, such as high hydrophilicity and stability to light or heat. Adsorption is commonly used as a technique for removing dyes. Removal of cationic dyes by adsorption is a promising approach because of its low performance cost and easy technical access. The amount adsorbed of the dye onto the polymeric resin is studied with time for estimating the adsorption mechanism. The adsorption of dye with time shows that mixing period of 10 min is optimum for attaining equilibrium with respect to R1 and R2, while attaining equilibrium with R3 takes 60 min. This findings represent a rapid kinetic for adsorption of MB, particularly R1, on the prepared resins. Different kinetic models were applied on the obtained results and the kinetic parameters were determined. The kinetic models correlate the amount adsorbed of dye with time. The values of calculated adsorption capacity q_e and the linear regression coefficient clarify that the studied kinetic model could not fit with the experimental results for adsorption of MB onto R1, R2, and R3. The results of the studied kinetic model clarify that the experimental results for adsorption of MB onto R1, R2, and R3 could be described by kinetic model supporting chemical adsorption. The sorption of MB could be favorably described by the pseudo-second-order kinetic model onto the composite resins. This finding refers to the participation of chemical adsorption within the adsorption mechanism for MB onto R1, R2, and R3.

Keywords: blue dyes, composite polymeric-apatite resins, cationic dyes, environmental purification

1. Introduction

The environmental issues associated with residual dye content or residual color in treated textile effluents are always a concern for each textile operator that

directly discharges, sewage treatment works as well as commercial textile operations to meet the requirements of color and residual dye imposed on the discharge of treated effluent [1]. In watercourses higher than 1.0 mg/L, dye concentrations induced by direct discharges of textile effluents, treated or not, can give rise to public enforcement. High concentrations of fabric dyes in water bodies halt the reoxygenation potential of the receiving water and cutoff sunlight, thereby disrupting biological activity in aquatic life as well as the aquatic plant or algae photosynthesis process [2]. Presence of dye is accepted as an esthetic issue in watercourses rather than as an eco-toxic hazard. The public appears to know the blue, green and brown color of the rivers, but the color 'non-natural' as red and purple usually causes the most concern. Due to their long-term existence in the environment (i.e., half-life of several years), accumulation in sediments and particularly in fish or other aquatic life forms, decomposition of contaminants in carcinogenic or mutagenic compounds, and also their low aerobic biodegradability, the polluting effects of dyes on the aquatic environment may also result in toxic effects. The majority of dyes are nonbiodegradable due to their artificial origin or chemical composition, possess carcinogenic activity, and induce asthma, dermatitis, inflammation of the skin, and various tissue changes. In addition, various azo dyes, primarily aromatic compounds, show toxicity both acute and chronic. High potential health risk is caused by adsorption of azo dyes and their breakdown products (toxic amines) through the gastrointestinal tract, body, lungs, and hemoglobin adduct formation as well as blood formation disturbance [3].

There are about 700,000 tons of colors, approaching 10,000 forms, often used as color operators in most of projects. The use of colors in characteristic media is disturbing considering their heavy workload, poisonous content, and bioaccumulative ability in living beings. In particular, the azo dyes that are most advertised and that cause cancer, need to be taken seriously. The current status of cationic and anionic dyes is audited here. For this reason, common adsorbents are commonly used, such as activated carbon, chitosan, composite, and natural waste. Various dangerous engineered dyes (cationic and anionic) have been fabricated with high creation rate. To dispose of their negative effects, the broad utilization of composite was watched for oxidative debasement/expulsion of colors from wastewater. In cationic dye, methylene blue, precious stone violet, Splendid Blue-R, and Rhodamine-B, while in anionic dye, Methyl orange, Congo red, Alizarin red S and Eosin Y, are broadly treated with composite.

Adsorption methods are used as procedures of high quality for the removal of dissolved organic contaminants from industrial wastewater, such as dyes. The fiber, pulp and paper industries are stated to use large quantities of a number of colors; such chemicals can be used in many wastewater factories that generating vast amounts of sprayed, toxic and even cancerous wastewater, causing serious hazard to aquatic living organisms. It is well known that dye effluents from the production of dyestuffs and fabric industries may have toxic effects on microbial organisms and may be toxic and/or cancerous to mammalian animals. Most of the dyes used in textile industries are resistant to light and not biodegradable. These are also resistant to aerobic digestion [4]. Because of simple design, adsorption has advantages over other methods and can entail low investment in terms of both initial and necessary land costs. The adsorption method is commonly used to treat industrial wastewater from organic and inorganic contaminants, and the researchers are paying close attention to it. The search for low-cost adsorbents with pollutant-binding capabilities has intensified in recent years. Locally available materials such as natural materials, agricultural waste, and industrial waste can be used as adsorbents at

low cost. For groundwater and wastewater treatment, the activated carbon produced from these materials can be used as an adsorbent [5]. Natural hydroxyapatite derived from bio-waste, bovine and camel bones in general. To remove the natural hydroxyapatite, three separate methods are applied: thermal decomposition, subcritical water, and alkaline hydrothermal processes. Results from many physiochemical analyses have shown that all the methods used are capable of removing the organic compounds present in bovine bones and producing pure bioceramic hydroxyapatite with an average yield of 65% [6]. A composite material is made by consolidating at least two materials—frequently ones that have altogether different properties. The two materials cooperate to give the composite novel properties. In any case, inside the composite you can without much of a stretch differentiate the distinctive materials one from the other as they do not break up or mix into each other [7]. One of the biggest advantages of the composite is it can be formed into entangled shapes more effortlessly than most different materials. This gives fashion designers the versatility to build any form or structure. In addition, composites are light in weight, contrasted with most woods and metals, possess high strength, dimensional stability, and are nonmagnetic. Composites contain no metals; hence, they are not attractive. They can be utilized around touchy electronic gear. The absence of attractive impedance permits huge magnets utilized as a part of MRI (Magnetic Resonance Imaging) hardware to perform better. Composites are utilized as a part of both the hardware lodging and table. Also, the development of the room utilizes composite rebar to strengthen the solid dividers and floors in the healing center [8].

In this chapter, our team will investigate the performance of (polymer/hydroxyapatite) composite for removal of methylene blue as cationic dye from aqueous system.

2. Materials and methods

2.1 Synthesis of composite resins

Polyacrylonitrile co-acrylic acid apatite resins, P(AN-co-AA)-HAP, were synthesized by radical copolymerization in DMF solution in the presence of (BPO) as follows: In three-neck round flask equipped with nitrogen, thermometer, and mechanical shaker, AN and AA (mass ratio of 4:1) were dissolved in the DMF (mass ratio of total monomer to DMF 4:11) solution 1. Different types of as-prepared natural HAP produced from camel bone with appropriate amount were dispersed in DMF and sonicated for 30 min then added to solution 1 in the three-neck flask and stirred under nitrogen purging. The initiator BPO was transferred to the reaction mixture with weight ratio of total monomers of 1:450. The solution was stirred until all substances were completely dispersed and monomers dissolved. After passing nitrogen to the solution for 1 h, the polymerization was performed in an airtight device at 60°C for 3 h till complete polymerization. After complete polymerization, the obtained composite was washed several times with water and acetone to remove the residual monomers and initiators thoroughly. The final co-polymer-HAP composites P(AN-AA)-HAP were dried at 60°C till complete dryness and ground to the specified particle size.

Different types of the as-prepared natural HAP camel bone samples were used as follows:

Resin	HAP preparation temp. °C	HAP preparation gas	HAP content % in the composite
R1	700°C for N_2 and 900°C for CO_2 with surface area 122.56 m^2/g	Passing N_2 gas for 2 h (1 h for rising temperature to reach to desired temperature and 1 h for holding) then passing CO_2 gas for 1 h	14%
R2	500°C for N_2 and 900°C for CO_2 was surface area 94.88 m^2/g		
R3	900°C for N_2 and 900°C for CO_2 was surface area 124.35 m^2/g		

2.2 Sorption studies

The sorption experiments were carried out on solutions containing methylene blue dye with the prepared sorbents in batch as well as column techniques.

2.2.1 Batch experiments

Batch experiments were conducted with 100 ml of methylene blue solution of concentration 1×10^{-5} M in 250-ml stoppered bottles containing 0.1 g of the composite material at pH 5.5. The mixture was shaken by a mechanical water shaker thermostated at 25 ± 1°C (except when studying the effect of temperature). The parameters affecting the sorption process were studied by varying any one of the parameters and keeping the other parameters constant. These factors include composite particle size, equilibrium time, dose, temperature, and the initial metal ion concentration. The solid material was separated from solution by centrifuge and the dyes concentration in the solution was determined. Methylene blue was determined spectrophotometrically using UV-visible spectrophotometer.

The amount of dye retained in the solid phase (q_e) (mg/g) was calculated using this relation:

$$q_e = \frac{v}{m}(C_0 - C_e)\ \text{mg/g} \tag{1}$$

where v is the volume of aqueous solutions (ml), m is the weight of solid material used (g), and C_0 and C_e are the initial and equilibrium concentration (M) of MB dye.

The sorption of dye solution was calculated using the relation:

$$\text{Sorption\%} = \frac{C_0 - C_e}{C_0} \times 100 \tag{2}$$

The distribution coefficient (K_d) of the dye between the aqueous phase and the solid phase is calculated from the relation:

$$K_d = \frac{v}{m}\left(\frac{C_0 - C_e}{C_e}\right) \tag{3}$$

$$K_d = \frac{q_e}{C_e} \tag{4}$$

2.2.2 Column studies

Column studies were conducted using glass column of dimensions 20 cm length and 1.2 cm of internal diameter and 0.4 g of sorbent of particle size 30 mesh was introduced as slurry in the column. A 1000-ml solution containing 1×10^{-5} M of MB added sample was passed through HAP. All the experiments were carried out at room

temperature. The sample solution was collected after different volumes. Amounts of MB in each volume were determined using UV/VIS spectrophotometry. The breakthrough sorption capacity of HAP was obtained in column using the equation:

$$Q_e = \left[\frac{C_i - C_e}{m}\right] bv \tag{5}$$

where C_i and C_e denote the initial and equilibrium (at breakthrough) dye concentration (M) respectively. *bv* was the breakthrough volume of the MB solution in liters, and *m* was the mass of the adsorbent used (g).

Desorption of solutes from the loaded column was carried out by elution using (H_2SO_4 + H_2O_2), HCL, NaOH, CH_3COOH, $C_2O_4H_2$, and $C_6H_8O_7$. From the start of the experiment, effluent samples at different volumes were collected at the bottom of the column for analysis. The percentage desorption of solutes was obtained in column using the equation:

$$\text{Desorption } \% = \frac{C_e}{C_i} \times 100 \tag{6}$$

3. Results and discussions

This chapter is divided into four parts. The first one deals with characterization of the synthesized sorbent materials, R1. The second and third parts are concerned with the removal of MB dye respectively from aqueous solution by the investigated sorbents. Capacities of the sorbent materials for removal of the studied dye were investigated. The fourth part deals with column studies (**Figure 1**).

3.1 Characterization of the sorbent materials

3.1.1 X-ray diffraction (XRD), Fourier transform infrared (FTIR), and scanning electron microscopy (SEM) measurements

The IR-spectra revealed wide bands of H—O—H lattice water in the regions 1600–1700 cm^{-1} and 3200–3600 cm^{-1} and an [OH]— stretching mode band at 3350 cm^{-1} for HAP at physical activation at 500°C. The bands at 1097 cm^{-1} and 1029 cm^{-1} were assigned for $(PO_4)^{3-}$. Also the bands at 960, 603, and 562 cm^{-1} are due to $(PO_4)^{3-}$. The $(PO_4)^{3-}$ vibrational bands depend on the activation temperature. The sharpness of the peaks at 603 cm^{-1} and 562 cm^{-1} indicates a well crystallized HAP. Characteristic vibration bands of the C—O in the carbonate group were observed at 1418–1456 cm^{-1}. New peaks were observed for composite resin (R1) at 2006 cm^{-1} and peak of phosphate is slightly shifted to 1042, 592, and 560 cm^{-1}, while the loaded resin R1 with MB dye showed a broad peak of the phosphate at 560 cm^{-1} and the stretching mode of vibration for OH group was observed at 3340 cm^{-1} as shown in the spectra. As can be seen from the morphologies of particles in the SEM images, there is a distribution of small particles and large agglomerates. These agglomerates are consisted of very fine particles that are welded together and the powders displayed a significant level of agglomeration. Forty-point BET surface area analyses were done to study the effect of polymer on the surface area of the natural hydroxyapatite. The natural HAP surface area was found to be 122.56 m^2/g, while composite shaped reaches 218.48 m^2/g. The XRD analyses revealed straight base lines and sharp peaks confirming that hydroxyapatite was formed in all samples, and the produced calcium phosphate was well

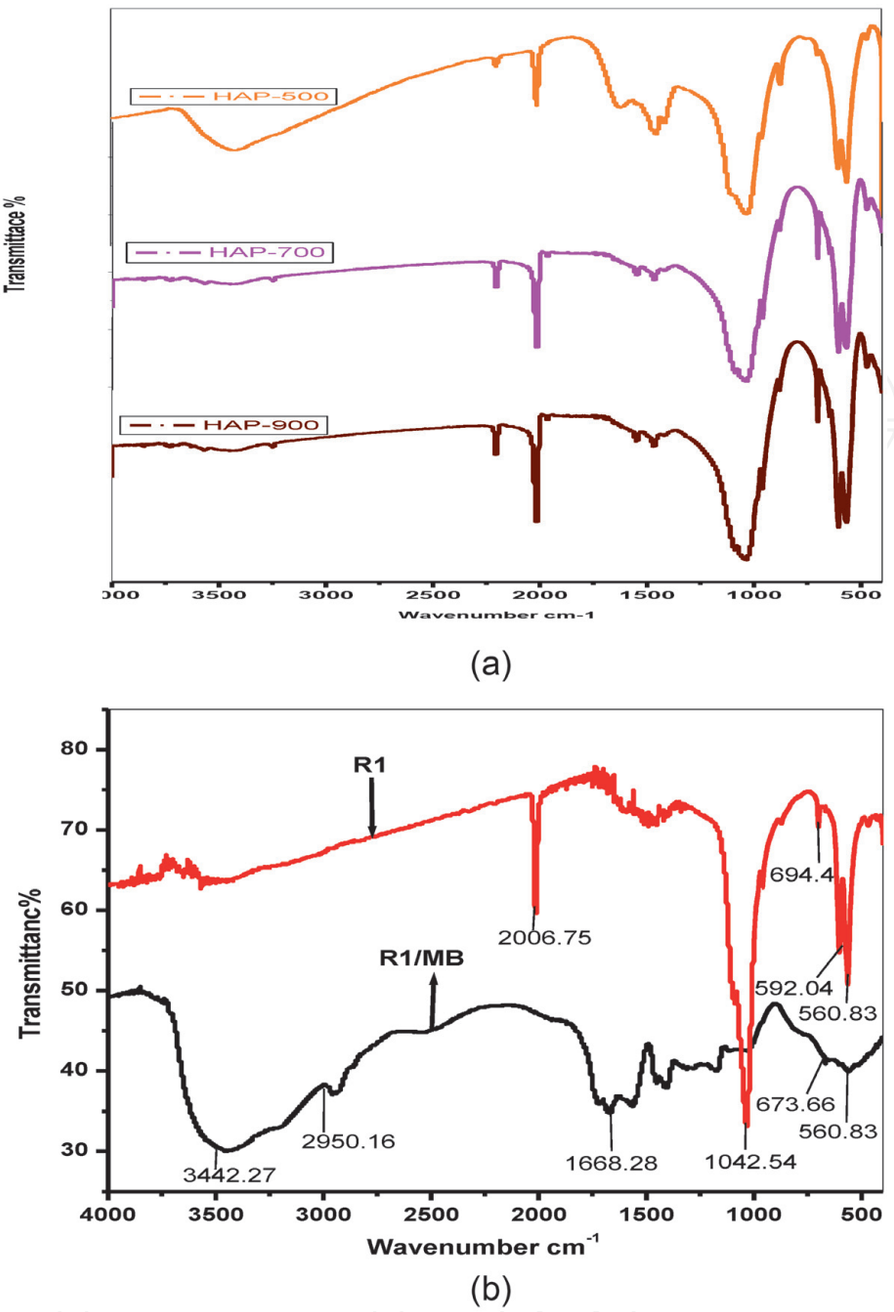

Figure 1.
(a) Infrared spectrum of the HAP samples and (b) infrared spectrum of the synthesized R1 and R1/MB.

crystallized. On the other hand, **Figure 2(a–c)** XRD analysis of HAP samples indicates that the samples are in the crystalline phase. In addition, XRD pattern shows a broad reflection peak at the range of 31.7–32.8 of 2 values, which correspond to the characteristic peak of hydroxyapatite. The XRD patterns of polymer/supported HAP composite resins with 14% HAP (R1) show that the characteristic peaks of HAP disappeared after the interaction between the polymer and HAP. This finding explains the interaction of the polymer within the HAP active groups (**Figure 3**).

3.1.2 Thermogravimetric analysis (TGA) measurements

The thermogravimetric analysis (TGA) measurements were performed in flowing nitrogen gas up on the prepared resins R1 as show in **Figure 4**. The thermal

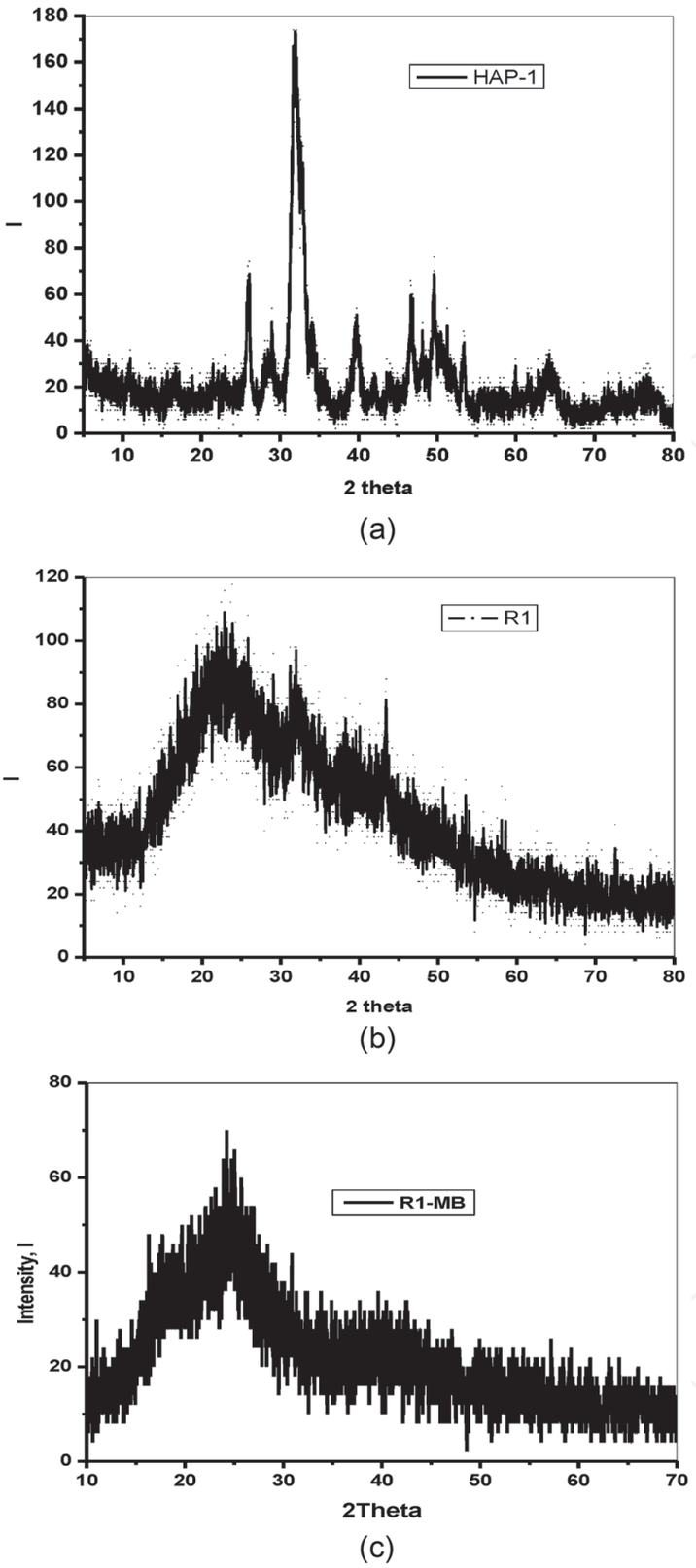

Figure 2.
(a) X-ray diffraction of the synthesized HAP, (b) X-ray diffraction of the synthesized R1, and (c) X-ray diffraction of R1 after sorption the of MB.

decomposition of the HAP-polymer composites illustrates that up to 350°C, 5 % weight loss occurred followed by three steps up to 800°C. It is clear that the presence of HAP with the polymer increases the thermal stability and delays the polymer thermal decomposition.

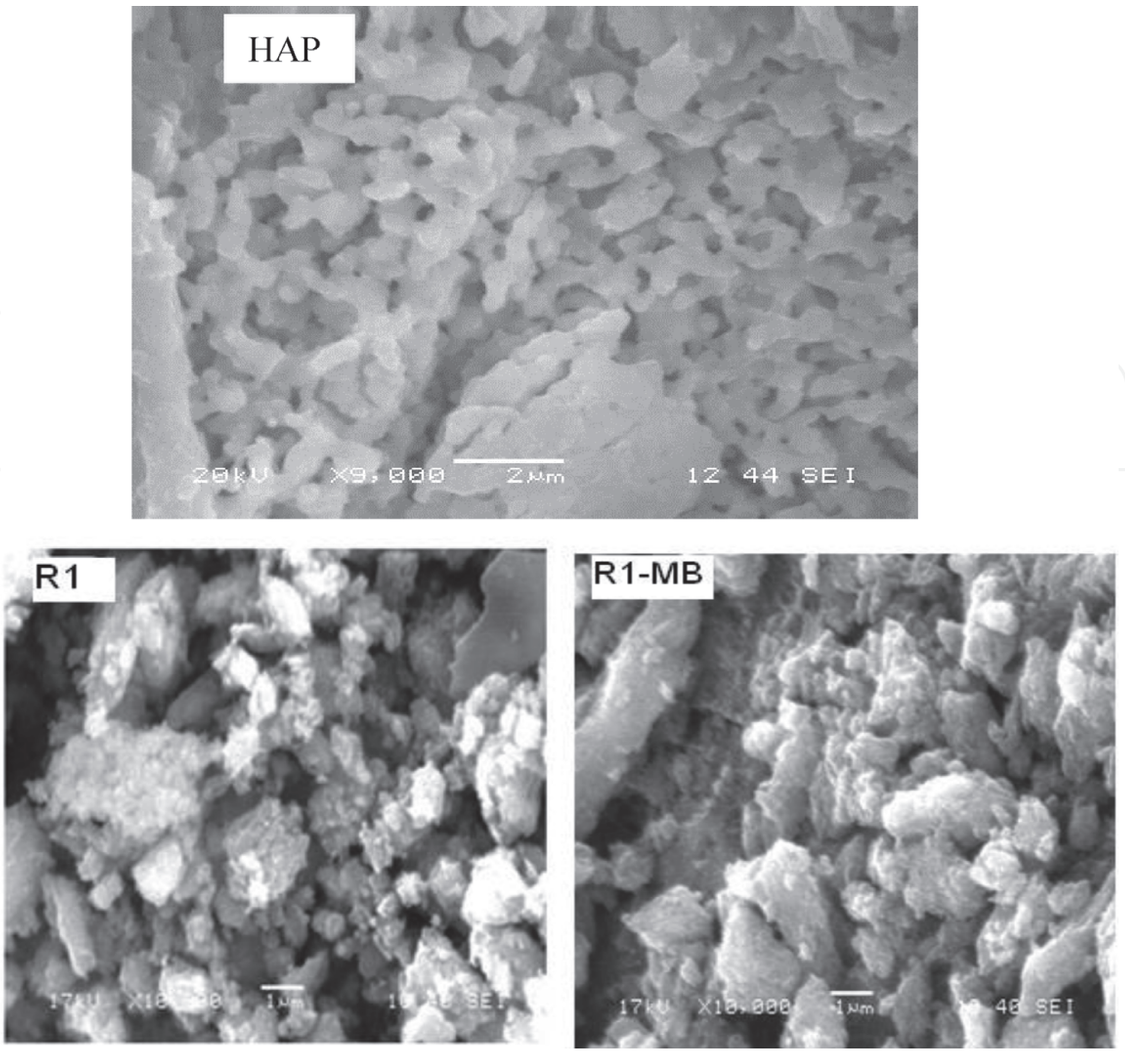

Figure 3.
SEM micrographs for the natural HAP and prepared resins before and after MB dye loading.

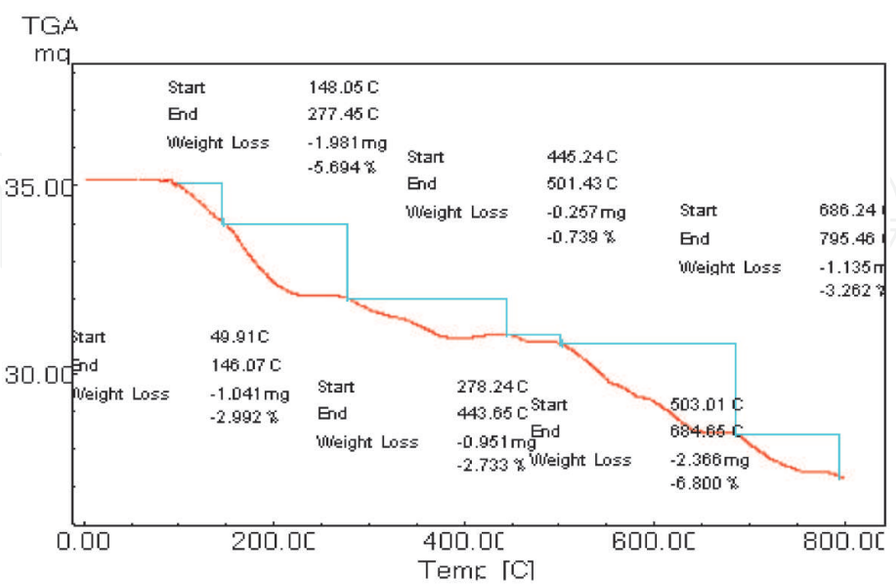

Figure 4.
TGA thermogram for R1.

The thermal decomposition of apatite content depends on its hydroxide and phosphate content; both are related to the change in apatite mass upon heating. After 800°C a replacement of —OH^- occurred, resulting in water evolution.

The weight loss after 800°C was attributed to the —OH^- content [9]. The calcium phosphates containing HPO_4 undergo weight loss between 400 and 700°C due to formation of pyrophosphate and evolution of water. It is reported that after 700°C the calcium pyrophosphate reacts with HAP to produce TCP and water.

3.2 Sorption investigations of methylene blue dye

3.2.1 Batch investigations

Batch experiments were carried out to find out the optimum conditions for the removal of MB dye from aqueous solution by the synthesized sorbents. Different parameters affecting the sorption of MB dye were separately studied, such as particle size of sorbent, shaking time, sorbent weight, temperature, and MB dye concentration.

3.2.1.1 Effect of shaking time

The effect of shaking time on the removal of 1×10^{-5} M MB dye from aqueous solution using 0.1 g of each the sorbents used was investigated in the range 1–120 min at 25 ± 1°C. The results illustrated in **Figure 5** show an increase in the removal percentage (uptake) of MB dye from aqueous solution with shaking time up to 60 min, which then remains constant with further increase of shaking time. A plateau is seen to be reached for all curves representing that the adsorbent is saturated at this time. Therefore, equilibrium time of 60 min was chosen in the subsequent studies.

3.2.1.2 Effect of particle size

The effect of particle size on the removal efficiency of 1×10^{-5}M MB dye from aqueous solution using 0.1 g of selected sorbents was studied at different sorbent particle sizes in the range (0.063–4) mesh at 25 ± 1°C, the removal of MB dye was found to increase from 22.39 to 82.5% as the sorbent particle size increased from (4–0.063) mesh, see **Figure 6**. The higher sorption with smaller sorbent particles may be attributed to the fact that smaller particles provide a larger surface area. Hence, selected sorbents with particle size of 0.063 mesh has been chosen for further experiments.

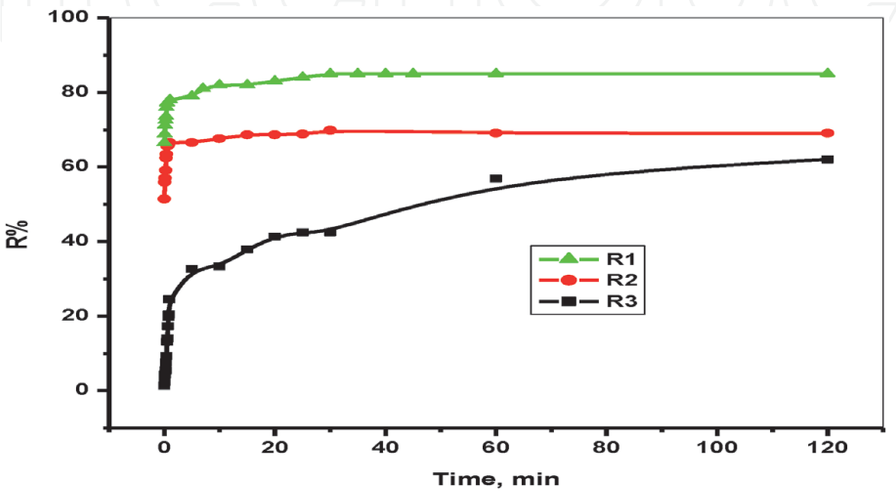

Figure 5.
Effect of shaking time on the adsorption of MB from aqueous solutions using apatite resins.

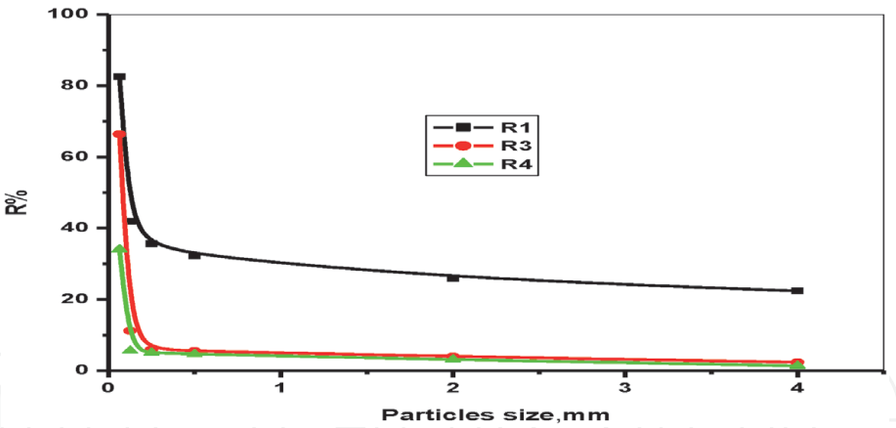

Figure 6.
Effect of particle size on the adsorption of MB from aqueous solutions onto apatite resins.

3.2.1.3 Effect of sorbent weight

The results for the removal of 1×10^{-5} M MB dye from aqueous solution using the investigated sorbents with respect to sorbents' weight are shown in **Figure 7** in the range 0.01–0.3 g/50 ml of 1×10^{-5} M MB dye solution at 25 ± 1°C. The results obtained show that when increasing sorbents' weight from 0.01 to 0.3 g, the removal of MB dye from aqueous solution increases and remains constant with further increase of sorbents' weight up to 0.2 g. This can be due to the availability of more surface functional groups and surface area at higher sorbent weight. The removal percentage of MB dye becomes constant from 0.2 to 0.3 g. This may be referred to the aggregation of the sorbent particles at high concentration of MB dye. Such aggregation would lead to decrease in the total surface area available for metal ion sorption.

3.2.2 Kinetics of adsorption

The amount adsorbed of dye onto the polymeric resin was studied with time for estimating the adsorption mechanism. The adsorption of dye with time shows that mixing period of 10 min is optimum for attaining the equilibrium with respect to R1and R2, while attaining the equilibrium with R3 takes 60 min. These findings

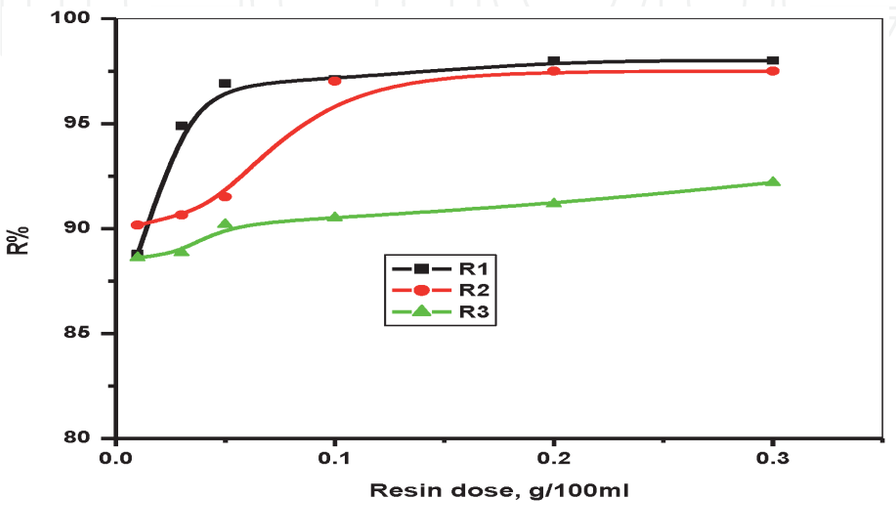

Figure 7.
Effect of resin dose on the adsorption of MB from aqueous solutions onto apatite resins.

reflect a fast kinetic for adsorption of MB onto the prepared resins, especially R1 and R2.

Different kinetic models were applied on the obtained results and the kinetic parameters were determined. The kinetic models correlate the amount adsorbed of dye with time. Lagergren presented the following equation for pseudo-first-order reactions [10]:

$$\frac{dq_t}{dt} = k_1(q_e - q_t) \tag{7}$$

where q_e and q_t are the dye concentration in solid phase at equilibrium and at time t, respectively, and k_1 is the model constant (min^{-1}). The linear form of the above equation was obtained by integration at the borders ($q_t = 0$ to $q_t = q_t$ and $t = 0$ to $t = t$) as:

$$\log(q_e - q_t) = \log q_e - \frac{k_1 t}{2.303} \tag{8}$$

The rate constant k_1 was determined from the plot of $\log(q_e - q_t)$ with t as shown in **Figure 8** while the value of q_e was determined from the intercept. The model variables with the coefficient are given in **Table 1**.

The plots in the figures above show linear fit with correlation coefficient (R) of 0.994 for R1. The values of calculated adsorption capacity q_e and the linear regression coefficient clarify that the studied kinetic model kinetic model could not fit with the experimental results for adsorption of MB onto R1.

Second-order kinetic model, which describes the chemical adsorption is given by [11].

$$\frac{dqt}{dt} = k_2(q_e - q_t)^2 \tag{9}$$

where k_2 is the model constant (g/mg min). The above equation could be integrated at the border ($q_t = 0$ to $q_t = q_t$ at $t = 0$ to $t = t$) to give:

$$\frac{t}{q_t} = \frac{1}{k_2 q_e^2} + \frac{t}{q_e} \tag{10}$$

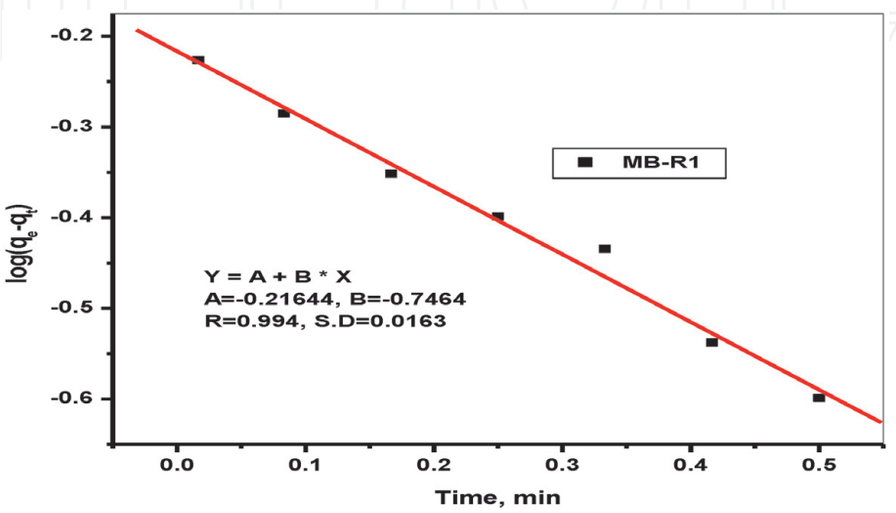

Figure 8.
Pseudo-first-order model kinetic plot for the sorption of MB onto the synthesized sorbents R1.

Adsorption system	Kinetic model	Parameters	R^2	SD
MB-R1	Pseudo first order	k_1 = 1.718 q_e = 0.607	0.994	0.0163
	Pseudo second order	K_2 = 2.18 q_e = 2.73	0.987	0.133
	Elovich	β = 5.98 α = 8.72	0.978	0.0376
	Intra-particle	k_{id} = 3.168 C = 2.93	0.991	0.834

Table 1.
Kinetic models' variables for adsorption of MB onto R1.

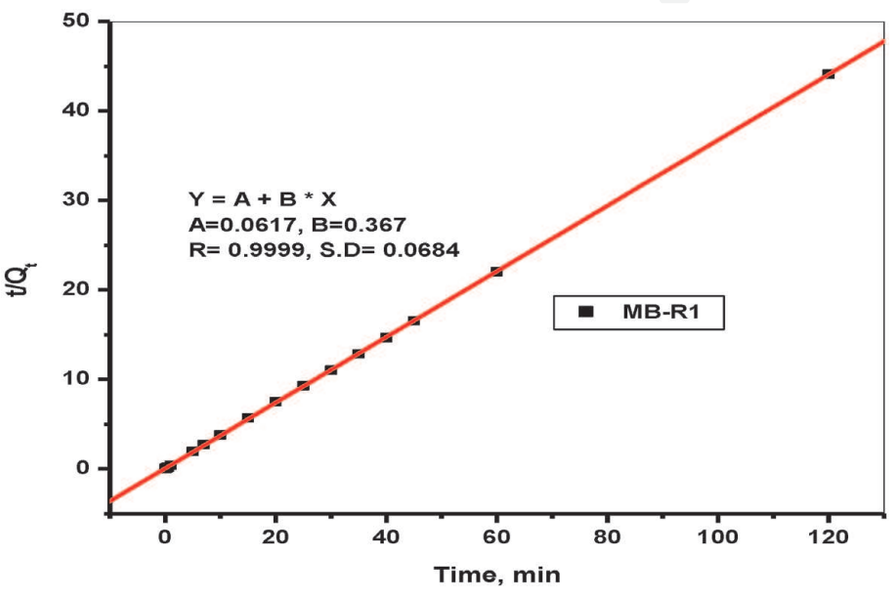

Figure 9.
Pseudo-second-order model kinetic plot for the sorption of MB onto the synthesized sorbents R1.

The model variables were calculated from the plot of t/q_t with t as shown in **Figure 9**. The plot showed a linear relation, and the model parameters with the correlation coefficient R^2 are given in **Table 1**.

The results of the studied kinetic model clarify that the experimental results for adsorption of MB onto R1, R2, and R3 could be described by kinetic model supporting chemical adsorption. The MB sorption could be represented favorably on the composite resins by the pseudo-second order kinetic model. This finding refers to the participation of chemical adsorption within the adsorption mechanism for MB onto R1.

Elovich kinetic model was applied upon the results to explain mainly the chemisorptions onto heterogeneous solid surfaces. The linearized form of Elovich model equation is given in [12].

$$q_t = \left(\frac{1}{\beta}\right) \ln(\alpha\beta) + \left(\frac{1}{\beta}\right) \log t \tag{11}$$

where α and β are model parameters representing the starting sorption rate (g mg^{-1} min^{-2}) and the leaching constant (mg g^{-1} min^{-1}), correspondingly. The model parameters were calculated from the linear fit of q_t vs. $\log(t)$ plot, shown in **Figure 10**, and are presented in **Table 1**.

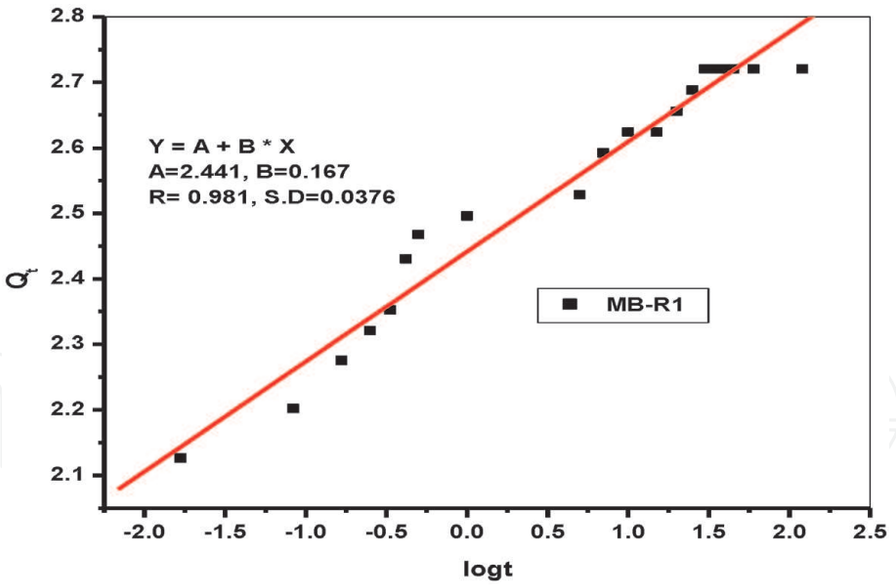

Figure 10.
Elovich model kinetic plot for the sorption of MB onto the synthesized sorbents R1.

The value of the Elovich constant (α and β) for the adsorption of MB on R1 predicate the effect of adsorbent dose and the possibility of performing sorption-desorption regeneration cycles of adsorbent. The value of correlation coefficient (R) reflects a poor fit of Elovich model with the experimental results. It could be inferred that both chemical and surface adsorption mechanisms are participating in the studied systems.

Intraparticle diffusion model was studied to explain the influence of transfer of dye from solution to solid surface of adsorbent on the reaction. The adsorption reaction could be affected by film diffusion, pore diffusion, surface diffusion, and/or adsorption on pore surface. The studied batch experiment was performed with shaking; therefore, the transfer of adsorbate particles could be described by diffusion coefficient that gives a considerable fitting with the experimental results. Weber model could be studied to explain the intraparticle diffusion's influence on the reaction by the following equation [13]:

$$q_t = k_{id} t^{0.5} + C \tag{12}$$

where k_{id} is the Webber model constant (mg g^{-1} $min^{-0.5}$) and C is a constant (mg g^{-1}) connected to the depth of the boundary layer, reflecting the boundary layer effect.

If the adsorption takes place within multilayer adsorbent, the adsorbate particles have to spread within the interior pores of solid materials. The model parameters were obtained from the plot of q_t vs. $t^{1/2}$, shown in **Figure 11,** and are presented in **Table 1**.

The results in **Figure 11** show two linear regions referring to the participation of at least two steps in the reaction. The linearity in the first region refers to a diffusion of dye into macro-pores of adsorbent, while the second linear region shows that the adsorbate particles diffuse within a micro-pore of adsorbent. The third region refers to mesoporous of adsorbent. The data obtained show that the synthesized sorbent has different pores.

The results in the figures reflect a variation of particle migration rate between different stages of sorption. The deviation of straight lines from the origin (when extrapolated), reflects that the diffusion within pore is not only the rate

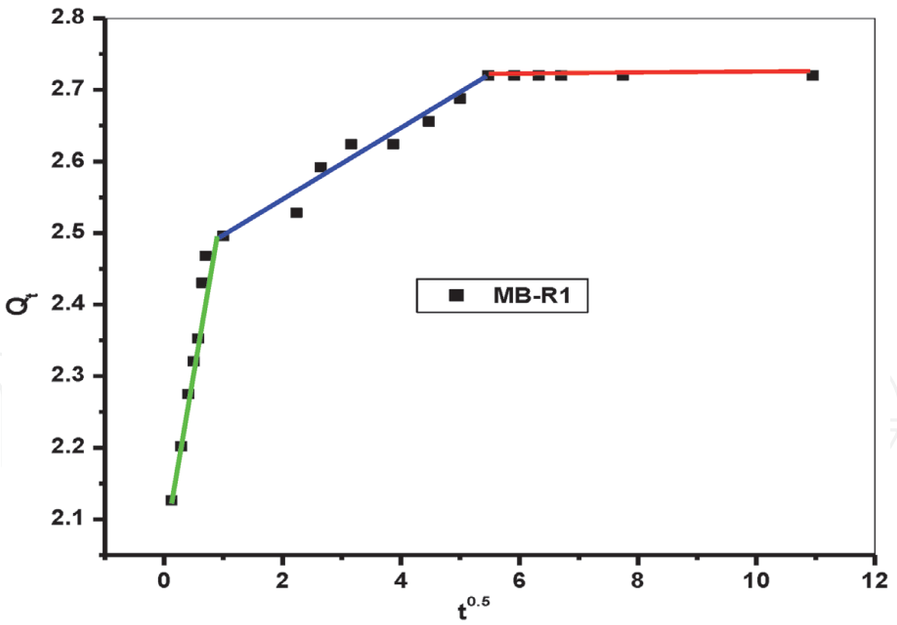

Figure 11.
Intraparticle model kinetic plot for the sorption of MB onto the synthesized sorbent R1.

determining step. The model variables for adsorption of MB using both R1, were given in **Table 1**. These results indicate that Webber diffusion model could not be considered as the controlling mechanism in the adsorption reaction.

3.2.3 Adsorption isotherm

The adsorption of MB onto R1 was studied at different initial dye concentrations (within the range 1–50 mg/L). The removal percentage and the adsorbed amount of MB are presented against the starting dye concentration in **Figure 12**. The results show that the amount of MB retained on the solid adsorbent increases with increasing dye concentration.

Different isotherm models were studied for describing the adsorption mechanism controlling the reaction. Langmuir isotherm model [13] was studied for adsorption of MB onto R1, which is expressed as:

$$\frac{C_e}{q_e} = \frac{1}{K_L} + \frac{C_e}{q_{max}} \tag{13}$$

where C_e is the dye concentration in solution after experiment (mg/L), q_e is dye concentration on the solid resin (mg/g), and q_{max} and K_L are model parameters connected to maximum adsorbed amount (mg/g) and adsorption energy, correspondingly. A plot of C_e vs. C_e/q_e is presented in **Figure 12** and the model variables were determined from the plot and are given with coefficient R in **Table 2**.

R values for the adsorption systems were found to be 0.975, indicating less compatibility with Langmuir isotherm. This finding prove that monolayer chemical adsorption on the homogeneous surface is not participate in the adsorption process.

Freundlich isotherm model [13] was applied on the experimental results, which is described by the equation:

$$\log q_e = \log k_f + \frac{1}{n} \log C_e \tag{14}$$

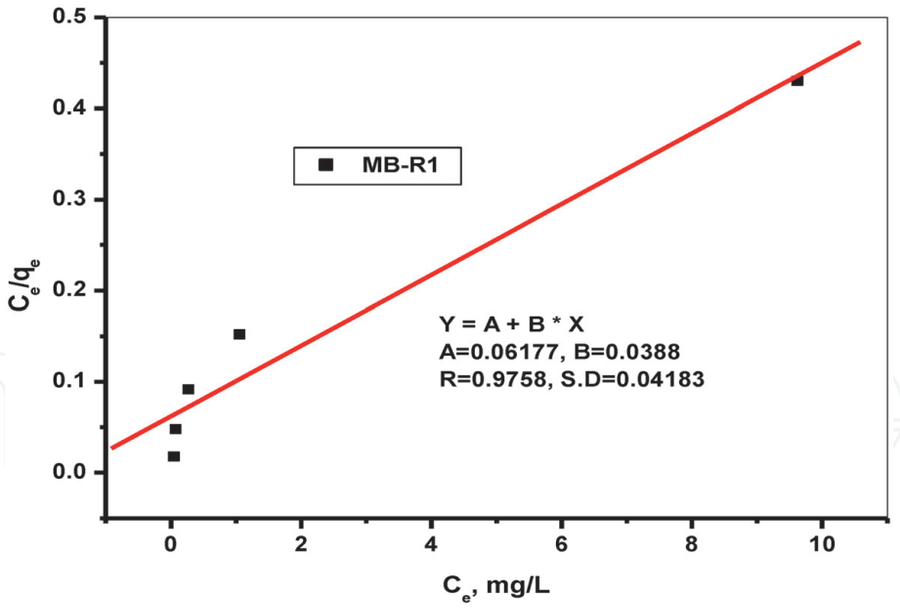

Figure 12.
Langmuir-1 isotherm plot for the sorption of MB onto the synthesized sorbent R1.

Model	Resin	Parameter	*R*	SD
Langmuir	R1	q_{max} = 25.77 K_L = 16.18	0.975	0.0418
Freundlich	R1	$1/n$ = 0.617 K_f = 6.102	0.988	0.104
Dubinin-Radushkevich	R1	β = −0.093 q_{max} = 10.39 E_S = 2.318	0.979	0.359

Table 2.
Adsorption isotherm models' parameters for MB-R systems.

where k_f (mg/g) and n are model constants, indicating the adsorption capacity and favorability nature of the adsorption process. Freundlich model constants were determined from the linear fit of log q_e vs. log C_e plot in **Figure 13** and are given with the correlation coefficient in **Table 2**.

The values of R of Freundlich plots for MB-R system showed bad fit of the experimental results with Freundlich isotherm model.

Dubinin-Radushkevich (D-R) adsorption isotherm model was studied; it describes adsorption onto porous solid surfaces, and is described by the following equation [13]:

$$\ln q_e = \ln q_{max} - \beta\varepsilon^2 \tag{15}$$

where β is the D-R model constant (mol^2/kJ^2), q_{max} is the constant referring to the maximum adsorbed amount (mg/g), and ε is Polanyi potential (ε = RTln(1 + 1/C_e)). The D-R model constants were obtained from the linear fit of the plot of ln q_e vs. ε^2 (**Figure 14**) and are given with correlation coefficient in **Table 2**. The adsorption free energy (E_S) is calculated as:

$$E_S = (-2\beta)^{-1/2} \tag{16}$$

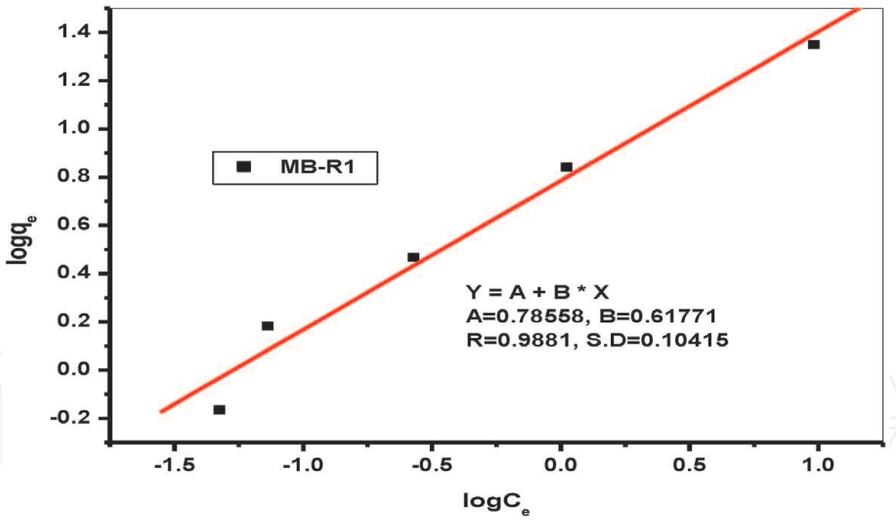

Figure 13.
Freundlich model isotherm plot for the sorption of MB onto the synthesized sorbent R1.

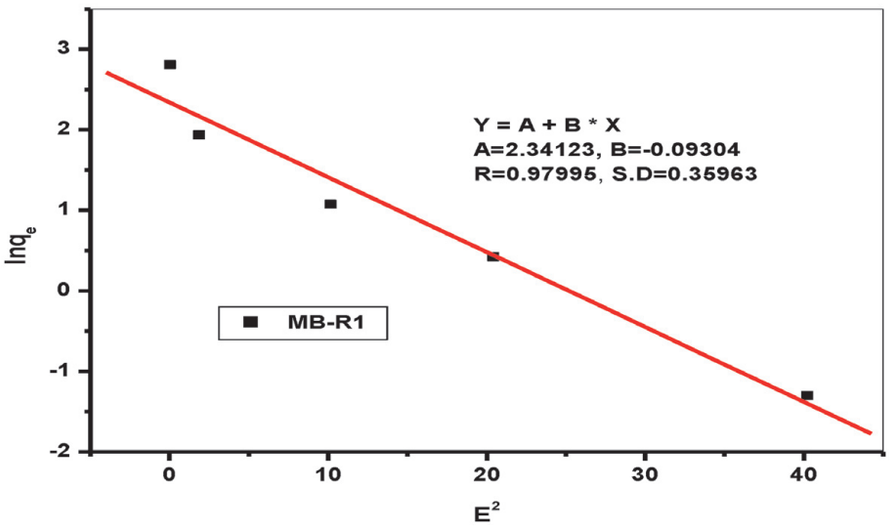

Figure 14.
Dubinin-Radushkevich model isotherm plot for the sorption of MB onto the synthesized sorbent R1.

The calculated mean adsorption free energy (E_S) from D-R model for adsorption of MB using R1 was found to be 8.03 kJ/mol. These values reflect that physical adsorption is a participating mechanism.

3.2.4 Effect of temperature

The effect of temperature on the removal efficiency of 1×10^{-5} M MB dye from aqueous solution using 0.1 g of each investigated sorbents was studied at different temperatures ranging from 25 to 50°C. It is observed from the results that the removal of MB dye increases slightly with increasing temperature, see **Figure 15.** This behavior indicates that the sorption process of MB dye from aqueous solution using all selected sorbents is an endothermic process. The increase in the sorption efficiency of MB dye by the sorbents used at high temperature may be attributed to the increase of MB dye mobility and decrease of the retarding forces acting on the diffusing dye.

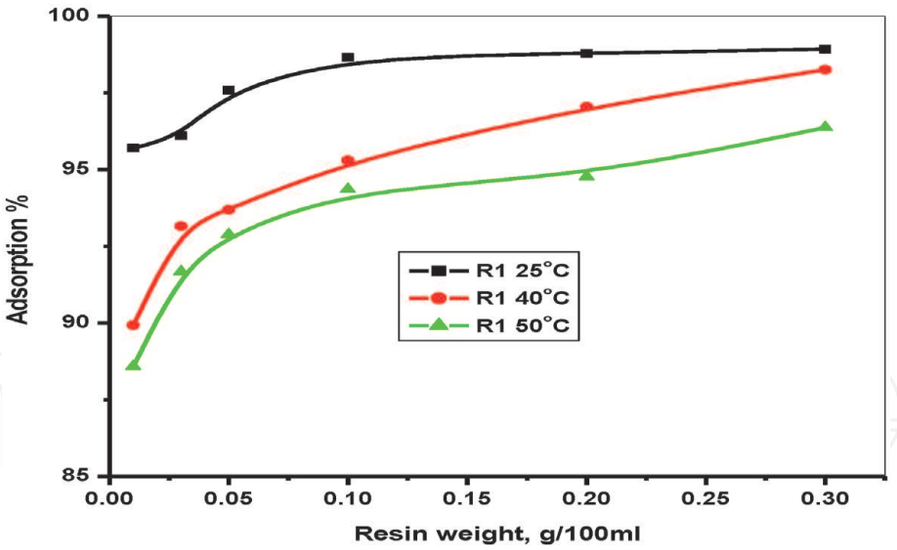

Figure 15.
Effect of temperature on the adsorption of MB from aqueous solution onto R1.

3.2.5 Adsorption thermodynamics

The thermodynamic parameters corresponding to dye sorption on the prepared resins were assessed using Van't Hoff equation [14] (**Table 3**).

$$\log K_d = \frac{\Delta S°}{2.303R} - \frac{\Delta H°}{2.303RT} \tag{17}$$

where k_d is the distribution coefficient of the solute ions, ΔS° is the entropy change (J mol^{-1} K^{-1}), R is the ideal gas constant (8.314 J mol^{-1} K^{-1}), and T is the absolute temperature. A plot of log k_d vs. $1/T$ was constructed as shown in **Figure 16** from which the slope of the straight line equal $-(\Delta H°)/2.303$; consequently, the value of apparent enthalpy change ($\Delta H°$) for the overall system was calculated. The values of other thermodynamic parameters are calculated at different temperatures, using the following equations:

$$\Delta G^{o} = -2.303RT \log k_d \tag{18}$$

$$\Delta G^{o} = \Delta H^{o} - T\Delta S^{\circ} \tag{19}$$

3.2.6 Column studies

Sorption dynamics of MB in a fixed bed flow through a sorption column is eventually conducted for multiple reuse of the sorbent. Column sorption studies of MB on the R1 beads at room temperature were investigated using aqueous solution

Adsorption system	Temperature (°K)	$\Delta H°$ (kJ mol^{-1})	$\Delta G°$ (kJ mol^{-1})	$\Delta S°$ (J K^{-1} mol^{-1})	SD
R1-MB	298	44.991	6.961	172.81	0.257
	313		−7.850		
	323		−11.626		

Table 3.
Thermodynamic parameters for sorption of MB onto R1.

of 1×10^{-5} M influent concentrations (C_i). Experimental breakthrough curve was studied using flow rate 0.2 ml/min. It is obtained by plotting the ratios of effluent concentration to initial concentration versus the volume of the effluent, see **Figure 17**. It was observed that the column gets saturated after passing 1 l of MB solution. The estimated breakthrough sorption capacity (Q_e) was 79.65 mg/g for MB.

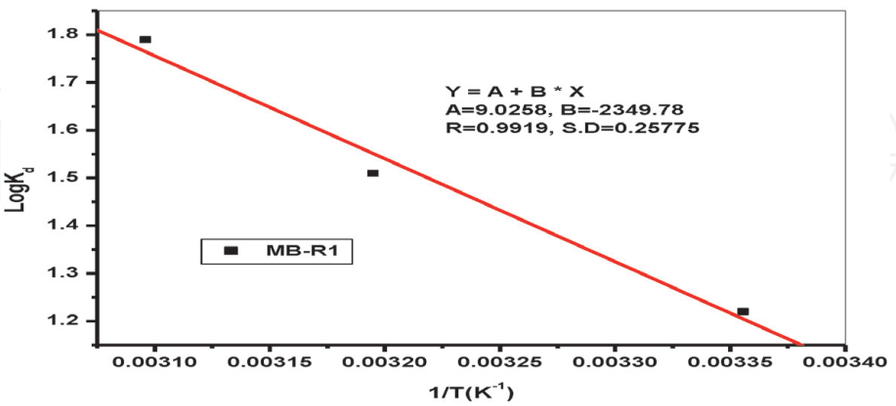

Figure 16.
Effect of temperature on the sorption of MB by the synthesized sorbent R1.

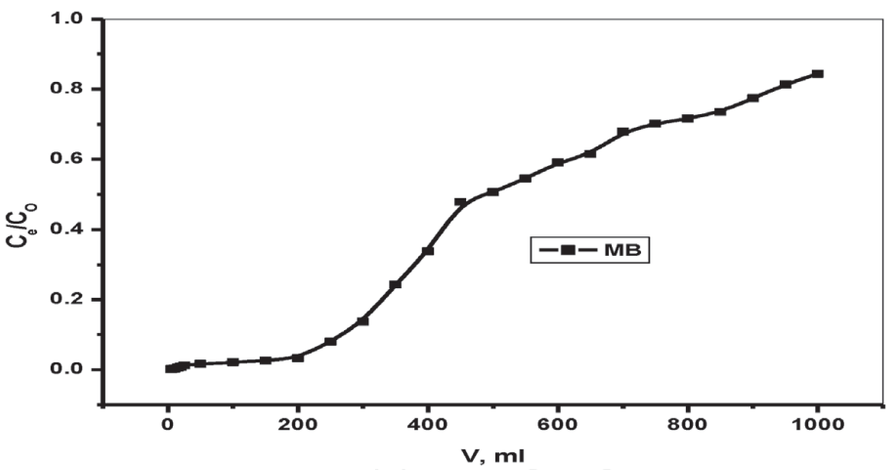

Figure 17.
Breakthrough curve of MB dye with R1.

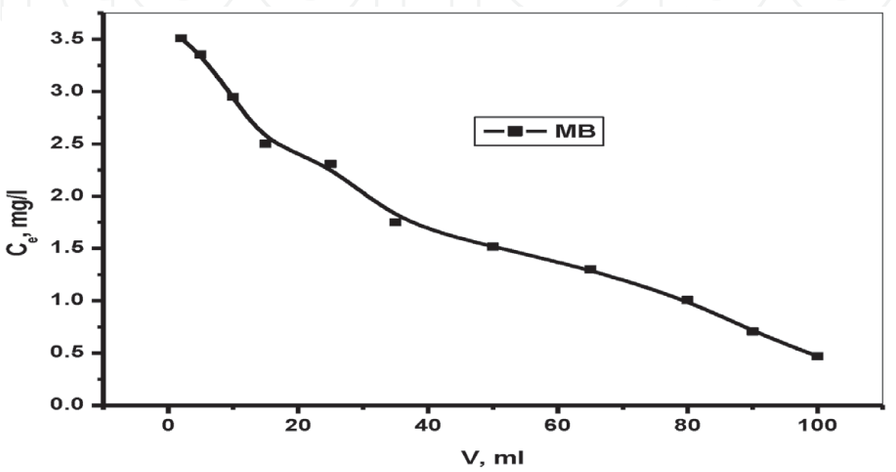

Figure 18.
Dynamic desorption curve of MB from R1 by H_2O_2 and H_2SO_4.

Once the column reached exhaustion, efficient elution of adsorbed solute from resin in column is essential to ensure the recovery of dye as well as the reuse of resin for repeated adsorption/desorption cycles. Desorption of MB from R1 was studied using different concentrations of sulfuric acid and hydrogen peroxide.

Desorption curve shown in **Figure 18** was obtained by plotting the effluent concentration (C_e) versus elution volume from the column at a flow rate of 0.2 ml/min. The result obtained shows that 93.79% recovery was achieved for MB by 1:1 W/W H_2SO_4 and H_2O_2.

4. Conclusions

In the current study, the removal of MB dye from aqueous solution was investigated by three prepared composite resins and the following conclusions can be drawn:

- The prepared composite resins can potentially be applied for removal of MB dye from aqueous solutions.
- The adsorption mechanism was suggested based on applying different isotherm models and kinetic models.
- From the data obtained for the uptake of MB dye by practical experiment, good match was found with calculated values obtained from isotherm models.
- Working on the composite is more advanced than working on HAP alone because:
    - The spontaneous reaction was carried out at low temperatures while HAP was carried out with spontaneous reaction at high temperatures.
    - The surface area and mechanical strength for composite are higher than the surface area and mechanical strength of HAP alone.
- Different inorganic and organic solutions were studied for regeneration of composite.
- Aqueous solution containing mixture of sulfuric acid and hydrogen peroxide of 1:1 w/w showed the maximum release for the adsorbed dyes with 87.46% for methylene blue dye.

Acknowledgements

The authors extend their appreciation to the Research and Development Grants Program for National Research Institutions and Centers (GRANTS) at King Abdulaziz City for Science and Technology (KACST) for supporting this work through research groups program under grant number 1-18-01-010-0002.

Author details

Nasser S. Awwad[1*], Adel A. El-Zahhar[1] and Jamila A.M. Alasmary[2]

1 Faculty of Science, Department of Chemistry, King Khalid University, Abha, Saudi Arabia

2 Faculty of Science for Girls, Department of Chemistry, King Khalid University, Abha, Saudi Arabia

*Address all correspondence to: aawwad@kku.edu.sa

References

[1] Zaharia C, Suteu C, Muresan A. Proceedings of International Conference on Environmental Engineering and Management. 2011;**4**:121

[2] Zaharia C, Suteu D, Muresan A, Muresan R. Environmental Engineering and Management Journal. 2009;**6**:1359

[3] Börnick H, Schmidt TC. J. Anal. Environ. 2006;**9**:181

[4] Doulati AF, Badii K, Yousefi Limaee N, Mahmoodi NM, Arami M, Shafaei SZ, et al. Dyes and Pigments. 2007;**73**:178

[5] Hassan SSM, Awwad NS, Aboterika AHA. Journal of Hazardous Materials. 2008;**154**:992-997

[6] Barakat NAM, Khila MS, Omrand AM, Sheikhd FA, Kima HY. Journal of Materials Processing Technology. 2009;**209**(2):3408

[7] El-Zahhar AA, Awwad NS. Journal of Environmental Chemical Engineering. 2016;**4**:633-638

[8] Awwad NS, Alshahrani AM, Saleh KA, Hamdy MS. Molecules. 2017, 1947;**22**(12). DOI: 10.3390/molecules22121947

[9] TÕnsuaadu K, Agris Gross K, Plūduma L, Veiderma M. Journal of Thermal Analysis and Calorimetry. 2012;**110**:647

[10] Lagergren S. Kungliga Svenska Ventenskapsakademiens Handlingar. 1898;**24**:1

[11] Ho YS, McKay E. Canadian Journal of Chemical Engineering. 1998; **76**:822

[12] Ho YS, McKay G. Science and Technology. 2002;**20**:797

[13] Dada AO, Olalekan AP, Olatunya AM, DADA O. Journal of Applied Chemistry. 2012;**3**:38

[14] El-Zahhar AA, Abdel-Aziz HM, Siyam T. Journal of Radioanalytical and Nuclear Chemistry. 2006;**267**(3):657